Appl Phys B (2008) 93: 749–752
DOI 10.1007/s00340-008-3272-3

Applied Physics B
Lasers and Optics

RAPID COMMUNICATION

Efficient generation of orange light in a quasi-periodically poled $LiTaO_3$ crystal

S.D. Pan · X.Q. Yu · Z. Yan · Y. Shen · X.J. Lv · S.N. Zhu

Received: 22 June 2008 / Revised version: 1 September 2008 / Published online: 31 October 2008

Abstract We present an approach to generating a tunable orange laser from 0.601 to 0.604 μm based on a quasi-periodically poled superlattice in $LiTaO_3$ and a Q-switched 1.064 μm Nd:YVO_4 laser as pump. The orange laser was generated in a cavity by a parametric process cascaded by a frequency mixing with a maximum output of 310 mW using 15 W pump power.

PACS 42.70.Mp · 42.79.Nv · 42.55.Xi

Light sources in the yellow range have many applications in biological technology, ophthalmology and display technology [1]. Commercial yellow lasers used in practice are mainly dye lasers, copper-vapor lasers and krypton lasers. These lasers are generally large in size and inconvenient in use. All solid-state lasers are of practical interest due to their compactness and efficiency. Strategies used to obtain visible output include frequency mixing of Nd-doped dual-wavelength lasers [2, 3], intracavity frequency doubling of Raman-shift lasers [4, 5], frequency doubling of infrared lasers [6, 7], and Raman shift from green to yellow using Raman crystal [8, 9], etc., in which the nonlinear crystals, such as KTP, LBO [4–7], or periodic poling optical superlattice, such as PPKTP, PPLN [2, 3], are usually used.

In this paper, we present a new approach to generating orange light using a quasi-periodically poled optical superlattice (QPOS) within a simple and robust Q-switched Nd:YVO_4 laser operating at 1.064 μm. Using a single QPOS, we were able to simultaneously obtain optical parametric oscillation (OPO), thus converting the 1.064 μm pump further into the infrared, as well as mixing of the residual pump with the OPO signal to obtain orange light. The visible emission was tunable within the wavelength range 0.601 to 0.604 μm as the operating temperature of QPOS was elevated from 150 to 195°C. A maximum output power of 310 mW was obtained, and the factors that influence the conversion efficiency are discussed.

Previously, we reported efficient frequency tripling using Fibonacci [10] and other quasi-periodical sequences optical superlattices [11]. Cascaded parametric interactions using general QPOS, to generate blue light from a laser of 0.532 μm, have also been reported [12, 13]. In the work presented here, the structure of QPOS is similar to that previously reported in [12]. Two building blocks in the superlattice, A and B, with widths D_A and D_B, respectively, were arranged in quasi-periodical sequence, as shown in Fig. 1. Each block contains a pair of antiparallel 180° ferroelectric domains, in which the positive domain possesses an equal width l. The reciprocal vector provided by the structure to compensate for phase mismatch is $G_{m,n} = 2\pi(m + n\tau)/D$, where $D = \tau D_A + D_B$ is the average structure parameter; m and n are two integers; and $\tau = \tan\theta$, where θ is the projection angle that determines the quasi-periodic order. The orange light we intended was at the wavelength of 0.602 μm. In order to use the largest effective nonlinear coefficient, $G_{1,1}$ was used for optical parametric generation (OPG) to generate a signal at the near-infrared and an idler at the mid-infrared, whereas $G_{3,2}$ was used for orange generation by mixing the signal and the pump. The Sellmeier equation of $LiTaO_3$ is provided by [14], and the phase matching temperature was set at 160°C. The structure parameters of the sample are: $D = 62.09$ μm, $\tau = 1.32$, $l = 6.91$ μm, $D_A = 23.02$ μm, $D_B = 32.45$ μm. With this structure, the

S.D. Pan · X.Q. Yu · Z. Yan · Y. Shen · X.J. Lv · S.N. Zhu (✉)
National Laboratory of Solid State Microstructures, Nanjing University, Nanjing 210093, People's Republic of China
e-mail: zhusn@nju.edu.cn
Fax: +86-25-83595535

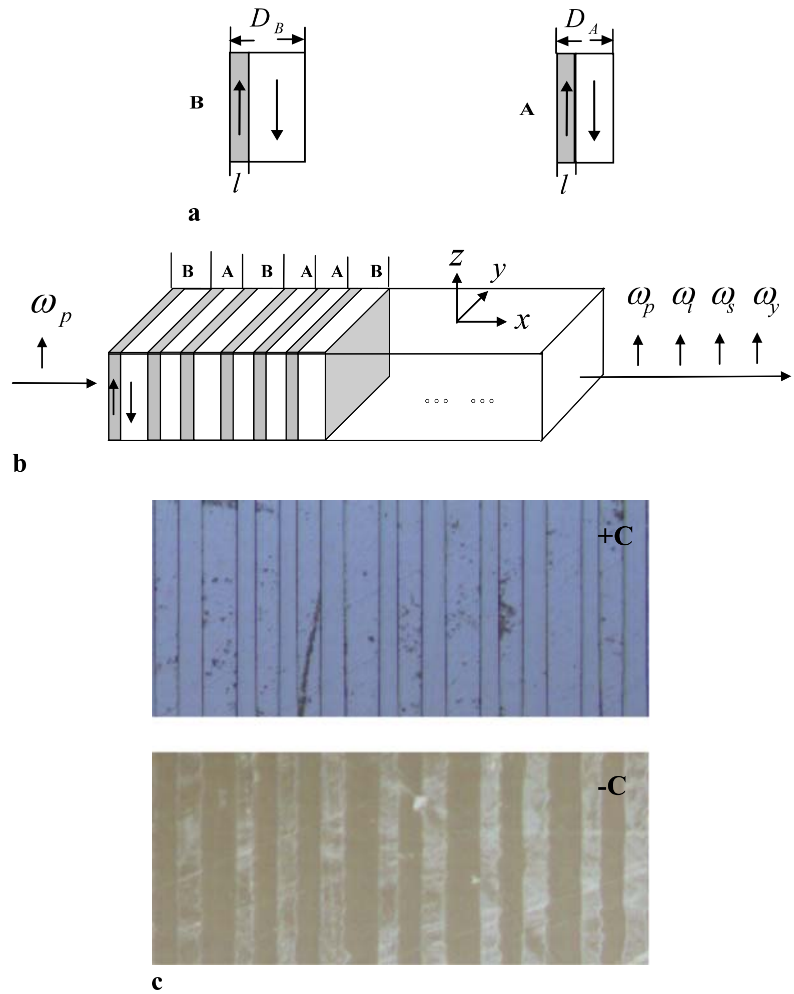

Fig. 1 QPOS made from a $LiTaO_3$ crystal. (**a**) Two building blocks, A and B, each composed of one positive and one negative ferroelectric domain. The *arrows* indicate the directions of spontaneous polarization. (**b**) A schematic diagram of the sample composed of two blocks, A and B, arranged in quasi-periodic sequence and the polarization orientation of electric fields in these two parametric processes with respect to the superlattice. (**c**) An optical micrograph of the etched domain-inverted patterns on the +C and −C surfaces

effective nonlinear coefficients of the QPM-OPG and QPM-SFG are $0.37d_{33}$ and $0.23d_{33}$, respectively, where d_{33} is the nonlinear coefficient of $LiTaO_3$. The two processes could be realized simultaneously in the superlattice and were coupled to each other. The pump at 1.064 μm was first transferred into the signal at 1.387 μm, then the orange at 0.602 μm continuously in every part of the QPOS. The sample was fabricated from a *z*-cut congruent $LiTaO_3$ wafer, which was 20 mm in length, 8 mm in width and 0.8 mm in thickness. Inverted domains were poled by conventional electrical poling technique [15]. Figure 1(c) is an optical photograph of etched domain patterns on the +C and −C surfaces. We can see that the inverted domains penetrate through the whole thickness of the sample and distribute uniformly.

Experimental setup is shown in Fig. 2. The pump source was a fiber-coupled diode laser (LD) emitting at 0.808 μm with a beam radius of 0.24 mm at the laser crystal. 1.064 μm laser light was obtained using a 0.3 at.% a-cut Nd:YVO_4 crystal with dimensions of 4 mm × 4 mm × 8 mm. Both faces were antireflection coated at 1.064 and 0.808 μm. The laser crystal was wrapped in indium foil and was mounted

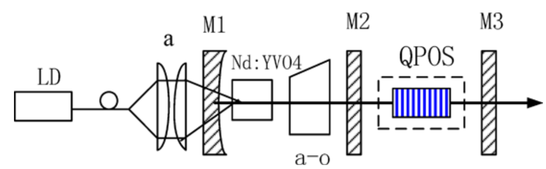

Fig. 2 A schematic of the experimental setup. LD: diode laser; a: coupling system; M_1, M_2, M_3: cavity mirrors; a-o: acousto-optical Q-switcher

in a water-cooled copper block. The water temperature was maintained at 20°C. An acousto-optical Q-switcher for 1.064 μm was inserted within the resonator after the laser crystal. The input concave mirror M_1, $R = 200$ mm, was antireflection coated at 0.808 μm and high reflection coated at 1.064 μm. The flat mirror M_2 was high transmission coated at 1.064 μm and high reflection coated at 1.387 μm. The flat mirror M_3 was high reflection coated at 1.064 and 1.387 μm and high transmission coated at 0.602 μm. The cavity length of the fundamental laser was 170 mm between M_1 and M_3. The cavity length between M_2 and M_3 was 60 mm. The QPOS sample was embedded in an oven

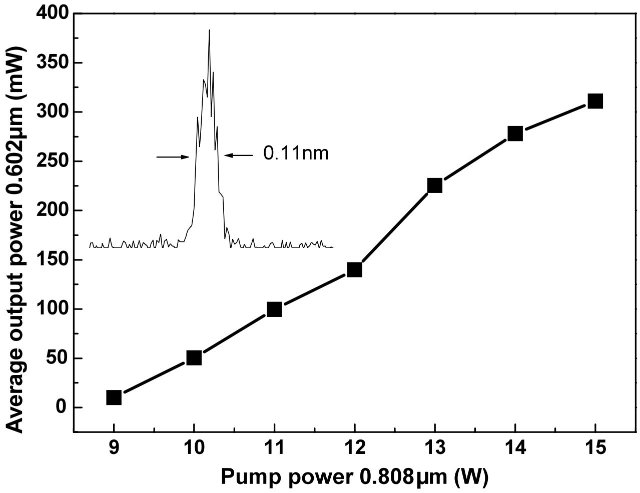

Fig. 3 The average output power at 0.602 μm with respect to incident pump power at 0.808 μm. The *insert* is a typical orange spectrum centered at 0.602 μm

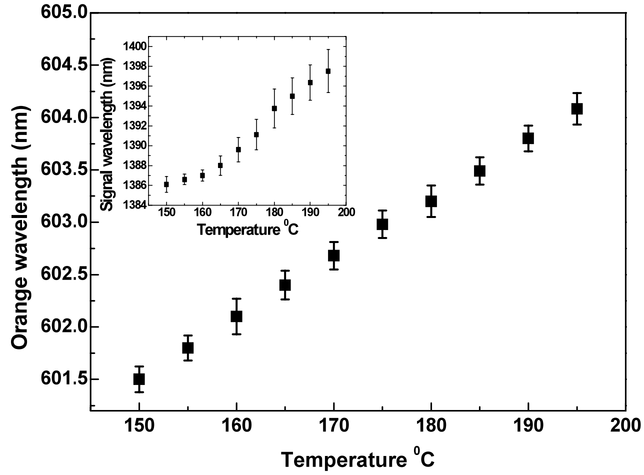

Fig. 5 Temperature dependence of orange and the corresponding signal wavelength (*insert*). The *error bar* indicates the FWHM at each measurement point

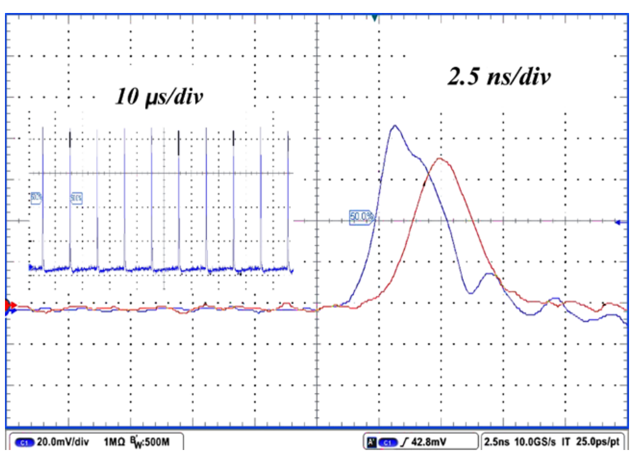

Fig. 4 Oscilloscope pulses of the orange at 0.602 μm and the leaked signal at 1.387 μm. The *insert* is the oscilloscope trace of the orange light at repetition rate of 10 kHz

(Model OTC-PPLN-20, Super Optronics Ltd.) with an accuracy of 0.1°C.

Figure 3 shows the average output power of orange light at 0.602 μm as a function of pump power at 0.808 μm. The insert is a typical spectra centered at 0.602 μm. The laser threshold was 7.9 W and the maximum output power was 310 mW with 15 W of pump power, corresponding to a slope efficiency of 4.3%. The pulse width of the orange and the corresponding signal were about 2.5 and 3 ns at the pump power of 15 W and repetition rate of 10 kHz, as shown in Fig. 4. The output pulses were monitored by a fast response InGaAs photo detector (New Focus 1623-AC) and digital oscilloscope (Tektronix TDS 5104). Correspondingly, the peak power and the pulse energy of the orange light were 12.4 kW and 31 μJ, respectively. As the pump power exceeded 15 W, the beam degraded and the orange light decreased rapidly, which may due to the visible-induced photorefractive effect of the crystal. The measured wavelength of the orange and the corresponding signal light were centered at 0.602 and 1.387 μm, respectively, at 160°C, which were consistent with the design. Figure 5 shows the measured orange and the corresponding signal wavelength as a function of temperature. The bars in the figure do not represent measurement error but stand for the bandwidth of the spectrum. The spectrum was recorded by optical spectrum analyzer (ANDO AQ-6315A). The center wavelength of the orange light varied from 0.601 to 0.604 μm as the QPOS temperature increased from 150 to 195°C , while that of the signal increased from 1.386 to 1.397 μm and the bandwidth from 0.57 to 2.17 nm. The orange light can hardly be observed when the temperature was lowered to 147°C. The bandwidth of the 0.602 μm and the corresponding 1.387 μm radiation were 0.11 and 0.57 nm, respectively. The narrower bandwidth of the orange light, which is determined by the bandwidth of the fundamental, signal and acceptance bandwidth of the superlattice, implies that only portion of the signal participated in the SFG process.

It is worthwhile to analyze the factors that hindered the conversion efficiency of the frequency conversion process in our experiment. First, the Fresnel reflection loss from the uncoated end faces of the QPOS is about 26%. It reduced the Q-value of the resonator, therefore increasing the threshold. The second one is due to the configuration of the concave-plan cavity we employed. The thermal lens of Nd:YVO_4 was >100 mm at pump power of ≤ 15 W. Taking into account the length of the superlattice, the average cavity mode diameter in the QPOS was >0.3 mm at the pump power of >2 W. Obviously, the focusing condition deviated heavily from the optimum value [16]. The third one is associated with the structure of the sample. The reciprocal space structure in a QPOS does not prevent conversion from other (non desired) QPM processes. For example, outputs at 1.306 and 1.617 µm, as well as the desired output at 1.387 µm, were detected at 160°C. These outputs correspond to other QPM-OPG processes in which the reciprocals $G_{4,-1}$ and $G_{-3,5}$ are involved. Since the Fourier component each of these is much smaller than that of the $G_{1,1}$, the light intensity at these signals were weaker than that at 1.387 µm. The energy transferred from the fundamental to either the 1.306 or 1.617 µm fields did not contribute to the generation of the orange light, but by contrast, decreased the conversion efficiency from fundamental to signal (at 1.387 µm) radiation. Finally, the non-perfect poling, including uneven and deviation in duty cycle from design, would have also resulted in the reduction in the overall conversion efficiency.

In summary, we have proposed and demonstrated, for what is to our knowledge the first time, the use of QPOS to generating orange light. A QPM-OPG cascaded by a QPM-SFG was achieved in a $LiTaO_3$ superlattice with quasi-periodical order. 310 mW orange light with 2.5 ns duration at 10 kHz repetition rate was obtained by using end-pumped intra-cavity optical parametric oscillation plus frequency mixing configuration. Tuning of the orange light from 0.601 to 0.604 µm was achieved by increasing the temperature of the QPOS from 150 to 195°C. The laser system has the advantages of simplicity, compactness and is wavelength tunable. In addition to quasi-periodic structure, dual-periodic and aperiodic structures can also be used for generating tunable orange light as long as the structure can provide two available reciprocals. In the same way, the QPOS crystal can be exploited in other wavelength ranges which are difficult to achieve in conventional nonlinear crystals in the birefringent phase matching scheme. Further work is under way.

Acknowledgements This work was supported by China Postdoctoral Science Foundation funded project (20070420997), by the National Natural Science Foundation of China (60578034, 10534020), by the National Key Projects for Basic Research of China (2006CB921804 and 2004CB619003), and by a grant from the National Advanced Materials Committee of China.

References

1. R.E. Fitzpatrick, Opt. Photonics News Nov. **6**, 24 (1995)
2. Y.F. Chen, Y.S. Chen, S.W. Tsai, Appl. Phys. B **79**, 207 (2004)
3. Y.F. Chen, S.W. Tsai, S.C. Wang, Y.C. Huang, T.C. Lin, B.C. Wong, Opt. Lett. **27**, 1809 (2002)
4. S.T. Li, X.Y. Zhang, Q.P. Wang, X.L. Zhang, Z.H. Cong, H.J. Zhang, J.Y. Wang, Opt. Lett. **32**, 2951 (2007)
5. P. Dekker, H.M. Pask, D.J. Spence, J.A. Piper, Opt. Exp. **15**, 7038 (2007)
6. S.M. Giffin, G.W. Baxter, I.T. Mckinnie, V.V. Ter-Mikirtychev, Appl. Opt. **41**, 4331 (2002)
7. I.T. Mckinnie, A.L. Oien, Opt. Commun. **141**, 157 (1997)
8. R.P. Mildren, M. Convery, H.M. Pask, J.A. Piper, T. Mckay, Opt. Exp. **12**, 785 (2004)
9. C. He, T.H. Chyba, Opt. Commun. **135**, 273 (1997)
10. S.N. Zhu, Y.Y. Zhu, N.B. Ming, Science **278**, 843 (1997)
11. C. Zhang, H. Wei, Y.Y. Zhu, H.T. Wang, S.N. Zhu, N.B. Ming, Opt. Lett. **26**, 899 (2001)
12. Y. Du, S.N. Zhu, Y.Y. Zhu, P. Xu, C. Zhand, Y.B. Chen, Z.W. Liu, N.B. Ming, X.R. Zhang, F.F. Zhang, S.Y. Zhang, Appl. Phys. Lett. **81**, 1573 (2002)
13. P. Xu, K. Li, G. Zhao, Y. Du, S.N. Zhu, Y.Y. Zhu, N.B. Ming, L. Luo, K.F. Li, K.W. Cheah, Opt. Lett. **29**, 95 (2004)
14. J.P. Meyn, M.M. Fejer, Opt. Lett. **22**, 1214 (1997)
15. S.N. Zhu, Y.Y. Zhu, Z.Y. Zhang, H. Shu, H.F. Wang, J.F. Hong, C.Z. Ge, J. Appl. Phys. **77**, 5481 (1995)
16. G.D. Boyd, D.A. Kleinman, Appl. Phys. Lett. **39**, 3639 (1968)